

On the impact of kinetic mixing in beta functions at two-loop

F. Lyonnet^{1,*}

¹*Southern Methodist University, Dallas, TX 75275, USA*

(Dated: November 5, 2018)

Kinetic mixing is a fundamental property of models with a gauge symmetry involving several U(1) group factors. In this paper, we perform a numerical study of the impact of kinetic mixing on beta functions at two-loop. To do so, we use the recently published PyR@TE 2 software to derive the complete set of RGEs of the SM B-L model at two-loop including kinetic mixing. We show that it is important to properly account for kinetic mixing as the evolution of the parameters with the energy scale can change drastically. In some cases, these modifications can even lead to a different conclusion regarding the stability of the scalar potential.

PACS numbers: 11.10.Hi,12.60.Cn,12.60.Fr

CONTENTS

I. Intro	1
II. Kinetic Mixing in PyR@TE	1
III. SM B-L	2
A. Lagrangian and symmetry breaking	2
B. Parameters and stability	3
IV. Effect of kinetic mixing at two-loop	3
A. Running of the parameters	3
B. Stability of the potential	3
C. Impact of \tilde{g}	5
D. Two-loop kinetic mixing contribution	6
V. Conclusion	7
Acknowledgments	7
References	7

I. INTRO

Renormalization group equations (RGEs) play a central role in studying the high-energy behaviour of extensions of the Standard Model (SM). The RGEs for an arbitrary gauge field theory at two-loop have been known for a long time [1–6] and their derivation for specific models has been automated in [7, 8]. An extra complication arises when the gauge structure contains multiple U(1) group factors as kinetic mixing can occur. This introduces $\frac{1}{2}n(n-1)$ extra dynamical parameters for each of which RGEs must be calculated. In addition, kinetic mixing induces modifications to the RGEs of the other parameters that also need to be taken into account for consistency. This work was carried out in [9, 10] for

the gauge couplings and extended in [11] for the dimensionless parameters at two-loop. Recently, an alternative method was presented in [12] in which the modifications to the RGEs for the dimensionful parameters are also derived. We implemented the method of [12] in the new version [13] of the computer code PyR@TE [7] which allows us to simply derive RGEs for a given model at two-loop taking into account kinetic mixing.

In this note we show that the impact of such kinetic mixing can be important for the high-energy behaviour of the theory parameters. To do so, we study the RGEs of the SM B-L model in which the SM has been supplemented by an additional U(1)_{B-L} group factor. We start in Sec. II by giving some details on how the kinetic mixing is implemented in PyR@TE. Sec. III summarizes the principle properties of the SM B-L model while Sec. IV is devoted to the study of the impact of kinetic mixing on the running of its parameters. Finally, our conclusions are presented in Sec. V.

II. KINETIC MIXING IN PYR@TE

Let's first consider a gauge field theory with n U(1) group factors $\mathcal{G} \times U(1)_1 \times U(1)_2 \times \dots \times U(1)_n$ where \mathcal{G} corresponds to the non Abelian part of the gauge structure. Gauge invariance then allows one to write the following term in the Lagrangian:

$$\mathcal{L} \supset \vec{F}^{\mu\nu} \xi \vec{F}_{\mu\nu}, \quad (2.1)$$

where ξ is an $n \times n$ symmetric matrix, and $F^{\mu\nu}$ is the vector of the n field strength tensors associated to the n gauge groups U(1)_{*i*}, $i = 1 \dots n$. This indeed introduces $\frac{1}{2}n(n-1)$ extra dynamical parameters. These additional parameters can be exchanged by corresponding *effective gauge couplings* that populate the off-diagonal entries of an extended gauge coupling matrix $G = \tilde{G}\xi^{-1/2}$ [12]. Of course the two approaches are equivalent and one can recover the results obtained working with ξ by performing suitable rotations.

The advantage of the effective gauge coupling method is that it does not require the introduction of new parameters ξ and their RGEs but only promotes the gauge

* flyonnet@smu.edu

Field	Quantum Numbers
Q_L	$(\mathbf{3}, \mathbf{2}, \mathbf{1}/\mathbf{6}, \mathbf{1}/\mathbf{3})$
u_R	$(\mathbf{3}, \mathbf{1}, \mathbf{2}/\mathbf{3}, \mathbf{1}/\mathbf{3})$
d_R	$(\mathbf{3}, \mathbf{1}, -\mathbf{1}/\mathbf{3}, \mathbf{1}/\mathbf{3})$
L_L	$(\mathbf{1}, \mathbf{2}, -\mathbf{1}/\mathbf{2}, -\mathbf{1})$
e_R	$(\mathbf{1}, \mathbf{1}, -\mathbf{1}, -\mathbf{1})$
ν_R	$(\mathbf{1}, \mathbf{1}, \mathbf{0}, -\mathbf{1})$
H	$(\mathbf{1}, \mathbf{2}, \mathbf{1}/\mathbf{2}, \mathbf{0})$
χ	$(\mathbf{1}, \mathbf{1}, \mathbf{0}, \mathbf{2})$

Table I: Particle content of the SM B-L model and their quantum numbers under $SU(3)_c \times SU(2)_L \times U(1)_Y \times U(1)_{B-L}$.

couplings to a non-diagonal matrix. The modifications due to kinetic mixing on the beta functions of the other parameters can be expressed as more or less complex replacement rules [12]. For instance one has

$$g^3 S(R) \rightarrow G \sum_p W_p^R (W_p^R)^T, \quad (2.2)$$

with $S(R)$ the Dynkin index of representation R . The sum p runs over all the fermions ($R = F$) or scalars ($R = S$). Finally, $W_i^R \equiv G^T Q_i^R$, with Q_i^R the vector of Abelian charges of the field i in the representation R . All the replacement rules derived in [12] have been implemented in the computer code PyR@TE at two-loop.

III. SM B-L

Our goal is to assess the size of the modifications due to kinetic mixing on the running of Lagrangian parameters. In order to do so, we will concentrate on the SM extended by an additional $U(1)_{B-L}$ group factor, i.e. B-L is promoted to a gauge symmetry. We will assume that we have an extra singlet scalar χ transforming as $\sim (1, 1, 0, 2)$ under $SU(3)_c \times SU(2)_L \times U(1)_Y \times U(1)_{B-L}$. In addition, we will consider three right-handed neutrinos $\sim (1, 1, 0, -1)$. This model has been extensively studied, in particular in the context of dark matter modeling, and constraints on the parameter space have been recently derived in [14].

A. Lagrangian and symmetry breaking

Table I list all the particles in the model along with their quantum numbers under $SU(3)_c \times SU(2)_L \times U(1)_Y \times U(1)_{B-L}$ gauge symmetry. Note that our setup is identical to [15].

With two scalars the most general scalar potential contains 5 parameters and reads

$$V(H, \chi) = \mu_H H^\dagger H + \mu_\chi \chi^\dagger \chi + \lambda_1 (H^\dagger H)^2 + \lambda_2 (\chi^\dagger \chi)^2 + \lambda_3 (H^\dagger H) (\chi^\dagger \chi). \quad (3.1)$$

The two scalars take the following vacuum expectation values (VEVs), leading to spontaneous symmetry breaking (SSB)

$$\langle H \rangle = \frac{1}{\sqrt{2}} \begin{pmatrix} 0 \\ v \end{pmatrix}, \quad \langle \chi \rangle = \frac{v'}{\sqrt{2}}. \quad (3.2)$$

The minimization conditions lead to the following expressions for v and v'

$$v^2 = \frac{\mu_\chi^2 \lambda_3 / 2 - \mu_H^2 \lambda_2}{\lambda_1 \lambda_2 - \lambda_3^2 / 4}, \quad (3.3)$$

$$v'^2 = \frac{\mu_H^2 \lambda_3 / 2 - \mu_\chi^2 \lambda_1}{\lambda_1 \lambda_2 - \lambda_3^2 / 4}. \quad (3.4)$$

After SSB, the two neutral scalars mix leading to two physical states of mass $m_{1,2}$. Defining the mixing angle between the two scalars, θ , one can derive the following relations [15]

$$\begin{aligned} \lambda_1 &= \frac{m_1^2}{4v^2} (1 + \cos 2\theta) + \frac{m_2^2}{4v'^2} (1 - \cos 2\theta), \\ \lambda_2 &= \frac{m_1^2}{4v'^2} (1 - \cos 2\theta) + \frac{m_2^2}{4v^2} (1 + \cos 2\theta), \\ \lambda_3 &= \sin 2\theta \left(\frac{m_2^2 - m_1^2}{2vv'} \right). \end{aligned} \quad (3.5)$$

There is an additional mixing angle, α , in the gauge sector which has been tightly constrained by LEP [16], $|\alpha| \leq 10^{-3}$, and the masses of Z and Z' bosons in this limit can be approximated by

$$M_Z \simeq \frac{v}{2} \sqrt{g_2^2 + g^2}, \quad M_{Z'} \simeq \frac{v}{2} \sqrt{\tilde{g}^2 + (4g'v'/v)^2}, \quad (3.6)$$

in which g_2 is the gauge coupling of the $SU(2)_L$ gauge group and $\begin{pmatrix} g & \tilde{g} \\ 0 & g' \end{pmatrix}$ are the Abelian gauge couplings in the

upper triangular basis which is linked to $G \equiv \begin{pmatrix} g_{11} & g_{12} \\ g_{21} & g_{22} \end{pmatrix}$ via the rotation

$$\tilde{G} = G \cdot \begin{pmatrix} \cos \phi & -\sin \phi \\ \sin \phi & \cos \phi \end{pmatrix}, \quad (3.7)$$

$$\cos \phi = \frac{g_{22}}{\sqrt{g_{22}^2 + g_{21}^2}}, \quad \sin \phi = \frac{-g_{21}}{\sqrt{g_{22}^2 + g_{21}^2}}. \quad (3.8)$$

Finally, the Yukawa interactions of the model are dictated by the following Lagrangian

$$\begin{aligned} -\mathcal{L}_Y &= Y_d^{ij} \bar{Q}_L^i H d_R^j + Y_u^{ij} \bar{Q}_L^i \tilde{H} u_R^j + Y_e^{ij} \bar{L}^i H e_R^j \\ &+ Y_\nu^{ij} \bar{L}^i \tilde{H} \nu_R^j + Y_N^{ij} (\nu_R^i)^c \nu_R^j \chi + \text{h.c.} \end{aligned} \quad (3.9)$$

After SSB this leads to the following mass term for the neutrinos

$$-\mathcal{L}_Y^\nu = \underbrace{Y_\nu^{ij} \frac{v}{\sqrt{2}} (\nu_L^i)^c \nu_R^j}_{M_d^{ij}} + \underbrace{\frac{1}{\sqrt{2}} Y_N^{ij} v' \nu_R^i \nu_R^j}_{\frac{1}{2} M_m^{ij}} + \text{h.c.}, \quad (3.10)$$

which requires $Y_\nu \sim O(10^{-6})$ for light neutrinos while $Y_N \sim O(1)$ for heavy right-handed neutrinos in the TeV range, see [15].

B. Parameters and stability

In the numerical analysis, we will neglect the Yukawa couplings, Y_e, Y_d, Y_ν , and retain only the top Yukawa coupling,¹ y_t . For simplicity, the right-handed neutrino Yukawa will be reduced to $Y_N^{ij} = \delta^{ij} y_N$.

For the numerical analysis, we select the following set of parameters

$$\mathcal{B} = \{\theta, M_{Z'}, M_m, g', \tilde{g}, m_1, m_2\}, \quad (3.11)$$

from which we derive initial values for $\{v', y_N, \lambda_1, \lambda_2, \lambda_3, \mu_H, \mu_\chi\}$. Indeed, v' can be extracted from Eq. (3.6) and the knowledge of $M_{Z'}$, g' and \tilde{g} ; y_N is obtained directly from Eq. (3.10) whereas the values of the quartic couplings $\lambda_1, \lambda_2, \lambda_3$ result from Eq. (3.5). Finally, the initial values for the Lagrangian mass parameter, μ_H and μ_χ are fixed via the minimization conditions, Eq.(3.3) and Eq.(3.4). The SM Higgs mass is identified with the physical scalar mass $m_1 = 126$ GeV.

It is well known, that the stability of the scalar potential is achieved by the following conditions [15]

$$\lambda_1 > 0, \lambda_2 > 0, 4\lambda_1\lambda_2 - \lambda_3^2, \quad (3.12)$$

which we will investigate in the next section.

IV. EFFECT OF KINETIC MIXING AT TWO-LOOP

The RGEs for the SM B-L as derived with PyR@TE have been given recently in [13] which we refer to for the full expressions and details. Our goal here is not to obtain precise conclusions regarding the physics of the model at hand. It is rather to quantify the impact of kinetic mixing one can expect in a physical situation on the running of the parameters. Therefore, we neglect the electroweak matching conditions as well as the scalar threshold corrections due to the heavy Higgs. These corrections would not affect our conclusions regarding the amplitude of the impact of the kinetic mixing. The initial values of all the parameters are set at the scale of the Z-boson mass, M_Z , and evolved to 10^{19} GeV using C++ routines as provided by the PyR@TE package.

A. Running of the parameters

To begin, we simplify the situation and select a scenario in which there is no mixing between the two scalars,

¹ Where y_t is third diagonal entry of Y_u^{33} .

i.e. $\theta = 0$. In addition, we set $\tilde{g} = 0$ and will investigate the effect of $\tilde{g} \neq 0$ later. Note that this does not correspond to neglecting kinetic mixing as it is generated automatically by radiative corrections. The mass of the new heavy gauge boson $M_{Z'}$ is set to 2.5 TeV which is in the ballpark of the recent exclusion limits derived in [14]. Finally, we set the mass of the heavy Higgs to 750 GeV. Note that the value of the input parameters are chosen to be representative of the situation but are not fine tuned in any way and the size of the effects obtained with different numerical values are very similar. This first benchmark point will be referred to as $\mathcal{B}_1 = \{0, 2500, 1000, 0.2, 0, 126, 750\}$, see Eq.(3.11) where the dimensionful parameters are given in GeV.

Fig. 1 shows the running of some of the parameters of the B-L model when the kinetic mixing is fully taken into account at two-loop or neglected. More specifically, the gauge couplings g_{11} and g_{12} , the quartic couplings $\lambda_1, \lambda_2, \lambda_3$ and the Yukawa couplings y_t and y_N are shown. On Fig. 2 we display the corresponding ratio of the beta functions including kinetic mixing over the beta functions neglecting kinetic mixing.

While the impact on the gauge couplings is somewhat limited to 1-3 % it reaches 2-6% for the Yukawa couplings at the GUT scale. For the quartic couplings, the change is dramatic and deserves some comments.

- (i) λ_1 actually goes to zero when the kinetic mixing is neglected, see Fig. 1, causing the ratio to blow up;
- (ii) λ_2 gets large kinetic contributions at one-loop of the form $\sim g^2\lambda$ and $\sim g^4$ coming from Λ_{abcd}^S and A_{abcd} in the notation of [3]. Moreover, there is a back reaction coming from the impact of kinetic mixing on λ_3 since $\beta_{\lambda_2} \sim 2\lambda_3^2$. These effects ultimately lead to a ratio of 1.5 at 10^{10} GeV;
- (iii) the kinetic mixing in λ_3 is such that it turns the sign of the beta function around, from negative to positive at a scale of about 10^8 GeV, ultimately leading to a positive λ_3 at a scale of 10^{12} GeV.

Therefore, as expected the impact of kinetic mixing is governed by the evolution of the off-diagonal effective Abelian gauge couplings, g_{12}, g_{21} . In Fig. 3, we show the running of these two gauge couplings with the energy. It is important to note that the values of these gauge couplings stay perturbative all the way up to the Planck scale and that the effects seen in the other parameters are not the result of extreme values of the gauge couplings.

B. Stability of the potential

As we have already seen, the impact of kinetic mixing can be quite large on the running of the different parameters. In this section, we investigate how this translates in terms of the stability conditions, Eq. (3.12).

Fig. 4, shows the stability condition $4\lambda_1\lambda_2 - \lambda_3^2$ with and without kinetic mixing for \mathcal{B}_1 . The difference in this

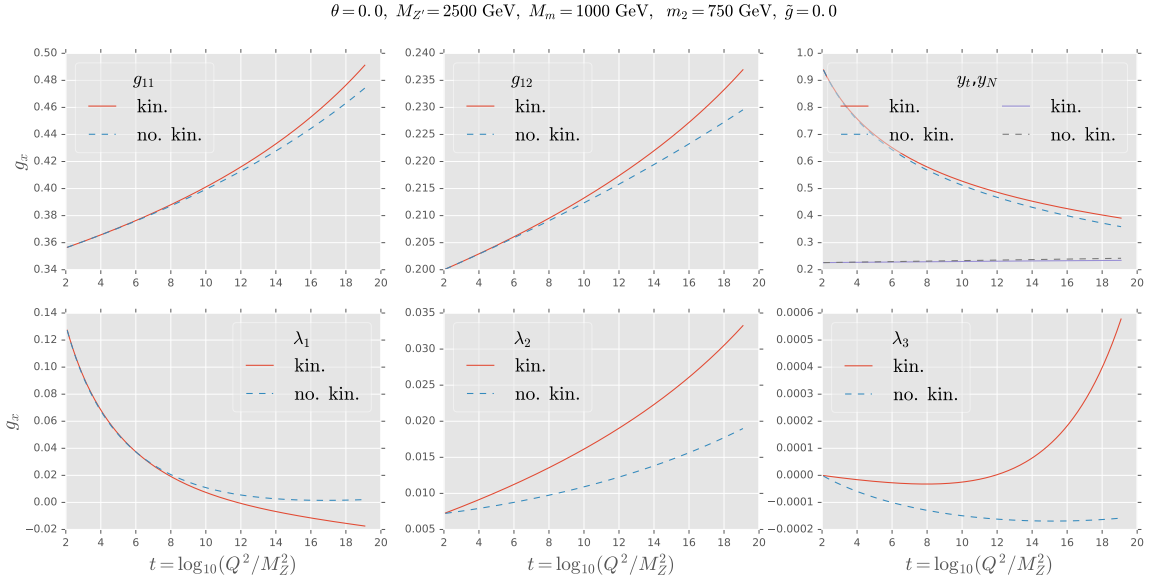


Figure 1: Running of the parameters in the B-L model in the case where the kinetic mixing is taken into account (solid lines) or neglected (dashed lines), for the benchmark point \mathcal{B}_1 . See text and figure title for the value of the input parameters. The parameters plotted are $g_1, g_{12}, y_t, y_N, \lambda_1, \lambda_2, \lambda_3$.

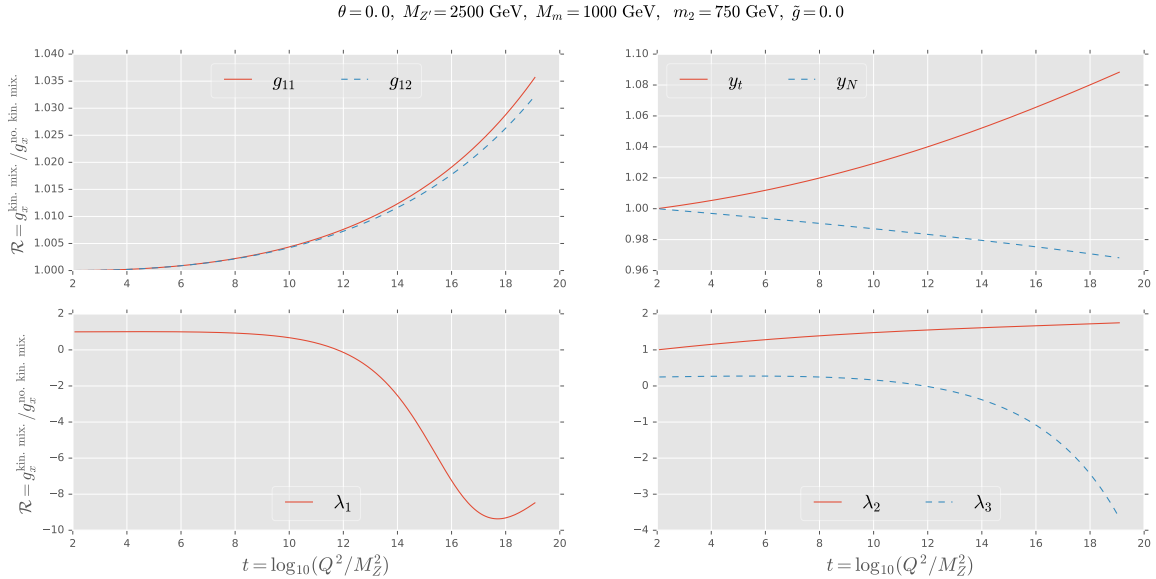


Figure 2: Ratio of the couplings taking into account or neglecting the kinetic mixing. The parameters plotted are $g_1, g_{12}, y_t, y_N, \lambda_1, \lambda_2, \lambda_3$. The initial values are those of \mathcal{B}_1 .

case is striking as the scenario develops an instability at around 10^{12} GeV when kinetic mixing is accounted for. This behaviour is actually simple to understand as the instability is the direct consequence of λ_1 turning negative at around the same scale, $\Lambda \sim 10^{12}$ GeV.

One might think that such a drastic change in results is limited to a small region of the parameter space, however that is not the case. Indeed, one can eas-

ily find regions where even the opposite situation happens, i.e. where the kinetic mixing *rescues* the stability of the potential. Fig. 5 shows such an example, for $\mathcal{B}_2 = \{0.1, 2500, 1100, 0.2, 0, 126, 800\}$. This scenario is the result of several competing effects.

- (i) $\theta \neq 0$ leads to $\lambda_3^{\mathcal{B}_2}(M_Z) \gg \lambda_3^{\mathcal{B}_1}(M_Z)$ which remains true at all scales, see Eq. 3.5.

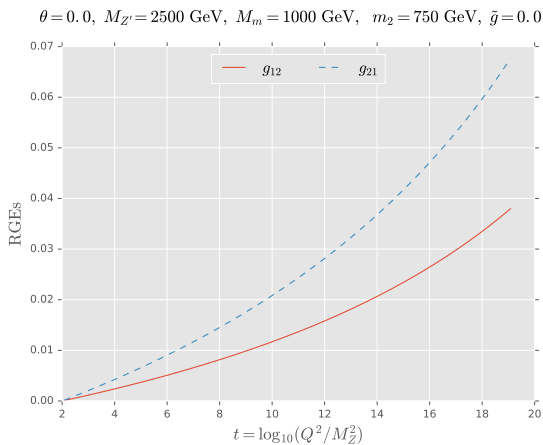


Figure 3: Running of the Abelian off-diagonal gauge couplings, g_{12} and g_{21} . The input parameters are the same as in Fig. 1.

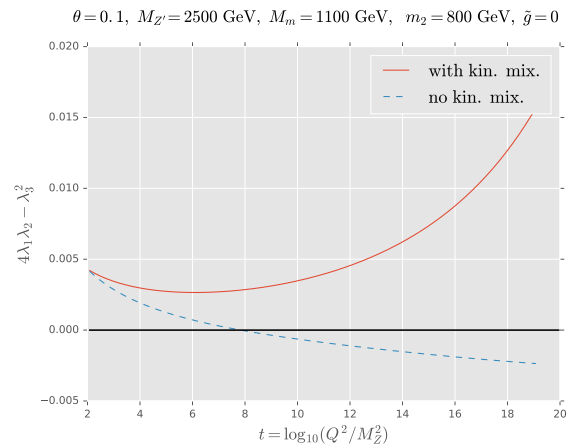


Figure 5: Stability condition for \mathcal{B}_2 . In this example, the kinetic mixing *rescues* the stability of the potential

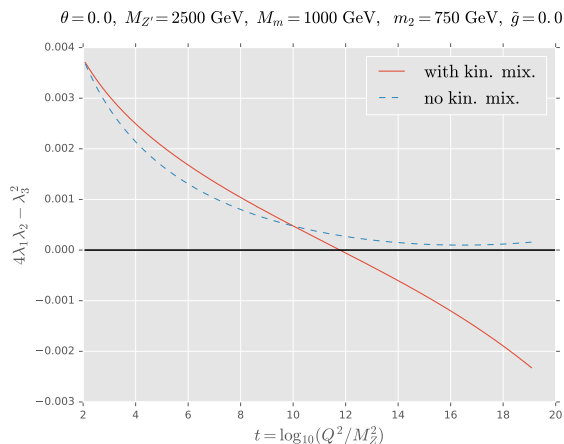


Figure 4: Stability condition for the benchmark point \mathcal{B}_1 of the B-L model in the case where the kinetic mixing is (solid line) or is not (dashed line) taken into account. The impact of kinetic mixing in this case leads to different conclusions.

(ii) $\lambda_1(M_Z) \sim m_2^2/(4v^2)(1 - \cos 2\theta)$, therefore $\theta \neq 0$ greatly increases $\lambda_1(M_Z)$ which leads to $\lambda_1 > 0$ at all scales.

(iii) Finally, λ_2 gets large kinetic corrections sufficient to overcome the increase in λ_3 .

One more thing to note is that the mass of the heavy Higgs plays a crucial role here. The initial values of $\lambda_{1,2,3}$ decrease with $m_2^2(M_Z)$ and for $m_2^2(M_Z) \sim 500$ GeV or lighter, λ_2 quickly runs negative without kinetic mixing leading to an unstable potential.

C. Impact of \tilde{g}

Finally, we investigate the impact of the value of \tilde{g} on the running of the parameters and the stability of the potential. To do so, we consider \mathcal{B}_1 but with $\tilde{g} \in \{0., 0.05, 0.1, 0.15\}$. The results are presented in Figs. 6 and 7 in which we show the running of the stability condition and the corresponding quartic couplings for different values of \tilde{g} respectively. Values of $\tilde{g} > 0.15$ will lead to non-perturbative couplings at the highest energies around 10^{19} GeV (not shown). The spread in $\lambda_{1,2}$ values, Fig. 7, due to different values of \tilde{g} is 35% and 15% respectively at the scale 10^{10} GeV while the λ_3 parameter is extremely small for $\tilde{g} = 0$ resulting in a spread of two orders of magnitude at the same scale.

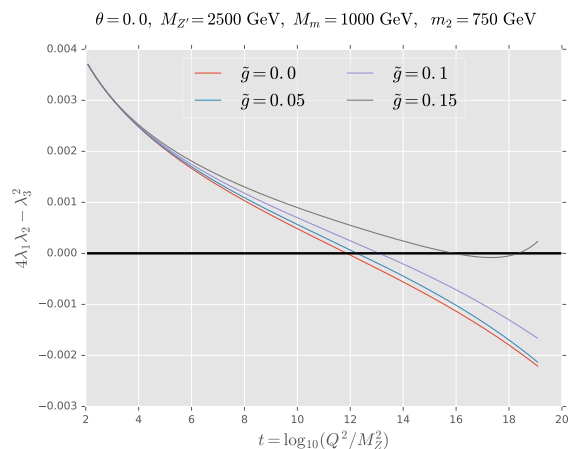


Figure 6: Stability condition in the \mathcal{B}_1 benchmark point for several values of $\tilde{g} \in \{0, 0.05, 0.1, 0.15\}$.

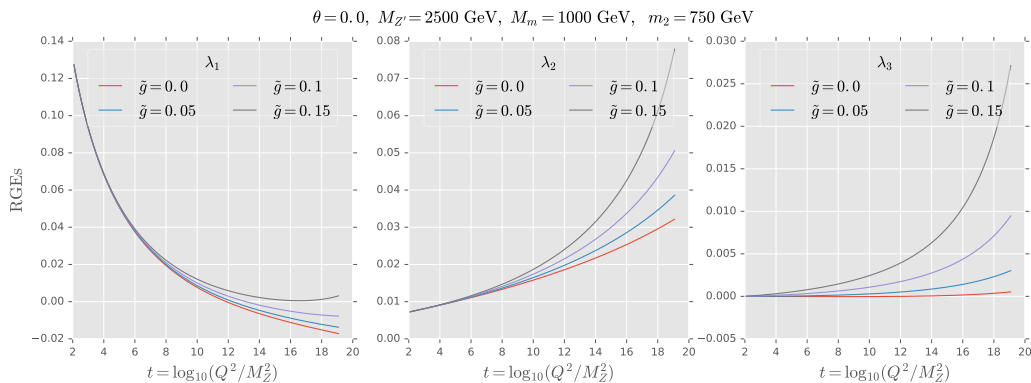


Figure 7: Running of the quartic couplings in the \mathcal{B}_1 benchmark point for several values of $\tilde{g} \in \{0, 0.05, 0.1, 0.15\}$.

D. Two-loop kinetic mixing contribution

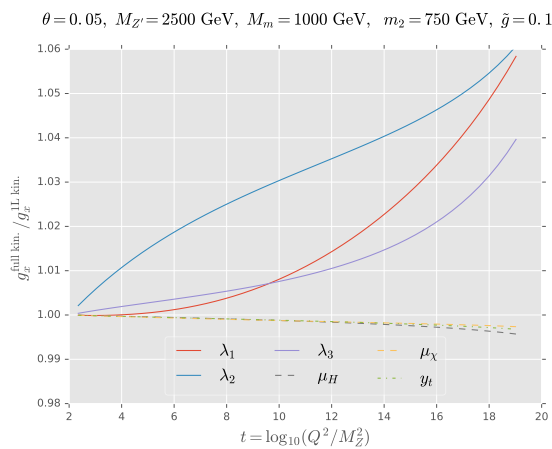


Figure 8: Running of some of the couplings of the B-L model for benchmark point \mathcal{B}_3 . We show the ratio of predictions including the full two-loop corrections coming from kinetic mixing over those including only the corrections up to two-loop order in the gauge couplings and one-loop elsewhere.

In this last part we focus on determining the amplitude of the kinetic mixing contributions at two-loop versus the one-loop order ones. To do so, we consider the two-loop beta functions without kinetic mixing to which we add either the two-loop, or one-loop order corrections coming from kinetic mixing. For simplicity, we keep the kinetic mixing contribution up to two-loop in the gauge couplings but switch on and off the two-loop order contributions in the other parameters. This would correspond to a simplified implementation of the rules of [12] in which the more involved replacement rules are ignored, and in particular the ones involving the scalar generators.

Fig. 8 shows ratios of couplings at two-loop as a function of the scale, in which the numerator is the coupling including the whole set of two-loop kinetic contributions, while the denominator is the same coupling in which only

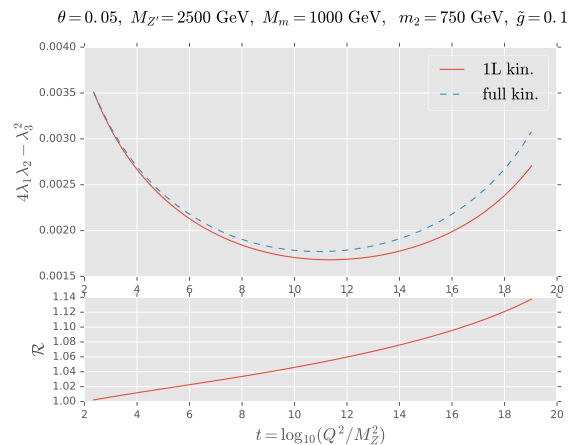


Figure 9: Stability condition in the B-L model for benchmark point \mathcal{B}_3 . We show the predictions including the full two-loop corrections (dashed line) coming from kinetic mixing and those including only the corrections up to two-loop order in the gauge couplings and one-loop elsewhere (solid line).

the one-loop kinetic mixing contributions have been retained². The benchmark point, \mathcal{B}_3 , used here is defined by $\mathcal{B}_3 = \{0.05, 2500, 750, 0.2, 0.1, 126, 1000\}$. The ratios are below 1% for the parameters μ_H, μ_χ and y_N , whereas for the quartic terms, they are typically larger than 1% at the scale 10^{10} GeV and can reach 5% at the GUT scale.

The corresponding effect on the stability condition, Eq.(3.12), are shown in Fig. 9. In the upper panel, the dashed line represent the stability condition in the case where all the corrections are included while the solid line is the result of retaining only the one-loop kinetic contribution. From the bottom panel, showing the ratio, it is easy to extract that the difference in the two approaches can be of the order 10%.

² Note that for the gauge couplings, the two-loop contributions are also taken into account.

While \mathcal{B}_3 is a particular point in the parameter space, it illustrates that neglecting the two-loop contributions coming from kinetic mixing might lead to an error of the order a couple of percents. In addition, it is not unlikely, that in some combinations of couplings like the stability condition of Eq.(3.12) these differences are enhanced leading to larger discrepancies. Furthermore, since contributions from the kinetic mixing terms and the base beta functions mix together, a coherent perturbative treatment at two-loop demands to take into account contributions coming from kinetic mixing at the same order.

V. CONCLUSION

Kinetic mixing is a fundamental property of models with an extended Abelian gauge structure like the SM B-L. Taking into account the kinetic mixing in the RGEs at two-loop is a complex procedure. To this end, we have consistently implemented the kinetic mixing at two-loop in the software PyR@TE. Therefore, these models now benefit from the same level of automation as their counterparts without kinetic mixing.

After reviewing the theoretical setup of the SM B-L, we studied in detail the impact of kinetic mixing on the running of the parameters of the model. We showed that

neglecting the kinetic mixing can lead to erroneous conclusions regarding the stability of the scalar potential. In addition, we studied the impact of the kinetic mixing contributions at two-loop and showed that they can be significant with respect to their one-loop counterparts.

Of course, our goal was only to illustrate that the features of a model can dramatically change when properly accounting for kinetic mixing; a careful treatment of the electroweak matching conditions and scalar threshold corrections would be required to draw detailed physical conclusions regarding the B-L model investigated here. We leave this to future work.

We believe that the order of magnitude of the effects exemplified with the SM B-L can be similar in other models and that taking kinetic mixing into account is crucial to obtain meaningful results. This is now a simple task thanks to PyR@TE.

ACKNOWLEDGMENTS

I would like to thank T. Jezo, A. Kusina, F. Olness, I. Schienbein, and F. Staub for their useful comments and for reviewing this manuscript. This work was also partially supported by the U.S. Department of Energy under Grant No. DE-SC0010129.

-
- [1] M. E. Machacek and M. T. Vaughn, “Two Loop Renormalization Group Equations in a General Quantum Field Theory. 1. Wave Function Renormalization,” *Nucl. Phys.* **B222** (1983) 83. I
 - [2] M. E. Machacek and M. T. Vaughn, “Two Loop Renormalization Group Equations in a General Quantum Field Theory. 2. Yukawa Couplings,” *Nucl. Phys.* **B236** (1984) 221.
 - [3] M. E. Machacek and M. T. Vaughn, “Two Loop Renormalization Group Equations in a General Quantum Field Theory. 3. Scalar Quartic Couplings,” *Nucl. Phys.* **B249** (1985) 70. ii
 - [4] I. Jack and H. Osborn, “Two Loop Background Field Calculations for Arbitrary Background Fields,” *Nucl.Phys.* **B207** (1982) 474.
 - [5] I. Jack and H. Osborn, “General Two Loop Beta Functions for Gauge Theories With Arbitrary Scalar Fields,” *J.Phys.* **A16** (1983) 1101.
 - [6] I. Jack and H. Osborn, “General Background Field Calculations With Fermion Fields,” *Nucl.Phys.* **B249** (1985) 472. I
 - [7] F. Lyonnet, I. Schienbein, F. Staub, and A. Wingerter, “PyR@TE: Renormalization Group Equations for General Gauge Theories,” *Comput. Phys. Commun.* **185** (2014) 1130–1152, 1309.7030. I
 - [8] F. Staub, “SARAH 4 : A tool for (not only SUSY) model builders,” *Comput. Phys. Commun.* **185** (2014) 1773–1790, 1309.7223. I
 - [9] F. del Aguila, G. D. Coughlan, and M. Quiros, “Gauge Coupling Renormalization With Several U(1) Factors,” *Nucl. Phys.* **B307** (1988) 633. [Erratum: *Nucl. Phys.*B312,751(1989)]. I
 - [10] F. del Aguila, J. A. Gonzalez, and M. Quiros, “Renormalization Group Analysis of Extended Electroweak Models From the Heterotic String,” *Nucl. Phys.* **B307** (1988) 571. I
 - [11] M.-x. Luo and Y. Xiao, “Renormalization group equations in gauge theories with multiple U(1) groups,” *Phys. Lett.* **B555** (2003) 279–286, hep-ph/0212152. I
 - [12] R. M. Fonseca, M. Malinský, W. Porod, and F. Staub, “Running soft parameters in SUSY models with multiple U(1) gauge factors,” *J. Phys. Conf. Ser.* **447** (2013) 012034. I, II, II, IV D
 - [13] F. Lyonnet and I. Schienbein, “PyR@TE 2: A Python tool for computing RGEs at two-loop,” 1608.07274. I, IV
 - [14] M. Klasen, F. Lyonnet, and F. S. Queiroz, “NLO+NLL Collider Bounds, Dirac Fermion and Scalar Dark Matter in the B-L Model,” 1607.06468. III, IV A
 - [15] C. Coriano, L. Delle Rose, and C. Marzo, “Constraints on Abelian Extensions of the Standard Model from Two-Loop Vacuum Stability and $U(1)_{B-L}$,” 1510.02379. III A, III A, III A, III B
 - [16] DELPHI Collaboration, P. Abreu *et al.*, “A Study of radiative muon pair events at Z^0 energies and limits on an additional Z' gauge boson,” *Z. Phys.* **C65** (1995) 603–618. III A